Building a suited reduced modal basis for updating 3D acoustic models with the Constitutive Law Error method

V. Decouvreur [a,1], A. Deraemaeker [b,2], P. Ladevèze [b]
Ph. Bouillard [a,*]

[a] *Structural and Material Computational Mechanics Dpt., Université Libre de Bruxelles, 50 av. F. D. Roosevelt CP 194/05, 1050 Brussels, Belgium*

[b] *Laboratoire de Mécanique et Technologie, ENS-Cachan Université Paris VI/CNRS, 61 av. Président Wilson, 94235 Cachan, France*

Abstract

We have recently reported the possibility of developing an updating technique for acoustic finite element models based on the constitutive law error proposed by P. Ladevèze and co-workers in structural dynamics. Like with every updating technique, we are confronted with and interested in reducing the computational time.
The main idea of this paper consists in building a reduced modal basis made of two contributions: static modes complete a truncated modal basis corresponding to the frequency range of computation. The static modes are associated to the system excitation (for instance a normal velocity boundary condition), but also to the system damping and to the reference measurements.
Updating acoustic models using the reduced modal basis shows a significant CPU-time saving with respect to the full non reduced system with an acceptable accuracy.

Key words: updating, validation, constitutive law error, model reduction, acoustics

* corresponding author
Email address: Philippe.Bouillard@ulb.ac.be (Ph. Bouillard).
[1] research fellow supported by the F.R.I.A. foundation (Belgium)
[2] presently: Active Structures Laboratory, Université Libre de Bruxelles, av. F. D. Roosevelt 50 CP 165/42, 1050 Brussels, Belgium

1 Introduction

In the last years, computer efficiency has increased fast, enabling us to manipulate very large models thanks notably to FEA codes running on a massively parallel architecture. For instance, the Salinas numerical prediction software was developed to run hundreds of millions of degrees of freedom (dofs) problems split among up to tens of thousands of processors with almost linear speedup factors (see Rohl and Reese (2000)). These complex heavy models describe generally quite well the geometry and allows us a higher frequency resolution of the problem. Nevertheless, the numerical simulation results are still somewhat too far from the recorded experimental data, which means that the model quality remains unsufficient. A possible solution for improving the model quality makes use of the experimental testing to update the numerical model.

The present paper uses a parametric updating technique based on the constitutive law error (CLE). The fundamentals of the CLE were first developed by P. Ladevèze in structural dynamics (see Ladevèze (1998)) and then applied to acoustics in Decouvreur et al. (2004). The main idea in the CLE technique consists in splitting the data and equations of the model into 'reliable' information and 'less reliable' one. Whether one trusts a given data or equation has to be related to the assumptions made in its derivation. The choice of the CLE updating technique among the different methods available in the literature is motivated in Decouvreur et al. (2004).

The updating process is iterative: each step consists in computing new updating parameters and solving the problem using these new values. The computed pressure is compared to the measurements using the constitutive law error, and the iterative process stops when the error is below a reference threshold value.

From a CPU-time point of view, an iterative process is very expensive since the same large model with different parameters has to be computed at each iteration to solve and to update the acoustic problem. From these considerations, large industrial setups can only be updated if the system size is reduced. In following sections, a reduced basis adapted to the updating of acoustic models with the CLE is formulated, assuming the knowledge of the excitations, the location of measurements, and the possible variations of the updated parameters. The reduced basis is made of a truncated modal basis to which Krylov vectors associated with the excitations are first added. The Krylov subspace technique is well known and largely investigated in the field of structural dynamics (Bui (2002)) or circuit simulation (Freund (2000)), and references therein. This basis is enriched by static corrections corresponding to forces located at the sensors and to the variable parameters. The building of such a reduced basis is explained and validated on a numerical example. The reason why this reduction technique is chosen among the other possibilities is that the present approach reduces the cost of updating the model drastically. Though,

there exist other reduction techniques. For instance, the multimodel approach builds a reduced basis made of truncated modal bases of the model for different values of the parameters (see Balmès (1996)). The following techniques are quite similar in principles to the one developed here: in Bouazzouni et al. (1997), the variation of the parameters of the model through the iterations is interpreted as excitations applied to the initial problem. Reduction techniques that are based on sensitivity vectors are other variants of this method (see Balmès (1998)). Other than using a reduced modal basis, there are alternative techniques, see for example the multipole expansion technique (Burnett (1994); Tournour and Atalla (1999)).
The paper is organized as follows: after describing the acoustic problem, the CLE principles are shortly summarized. The updating process is explained, together with the discretization of the acoustic problem. The construction of the reduced basis and its application to project the initial problem into a sub-space of lower size enables one to update a numerical example within a significantly lower computation time compared to the updating of the full model.

2 The CLE applied to acoustics

2.1 Principles

We are dealing with an acoustic problem defined on a domain Ω with boundary $\partial\Omega$. In linear acoustics, one assumes small harmonic perturbations of the particle velocity $\mathbf{v}$, the pressure p and the density ρ of the isotropic medium so that these oscillations around steady values are respectively written as follows:

$$\begin{cases} \mathbf{v} = \mathbf{v}' e^{j\omega t} \\ p = p' e^{j\omega t} \\ \rho = \rho' e^{j\omega t} \end{cases} \tag{1}$$

where $j^2 = -1$, ω is the angular frequency, and t the time.
The pressure field is the solution of the wave equation (called Helmholtz equation in the frequency domain) with associated Dirichlet, Neumann, and mixed Robin boundary conditions on parts $\partial_1\Omega$, $\partial_2\Omega$, and $\partial_3\Omega$ of the boundary respectively. These equations are given by (2).

$$\begin{cases} \text{Helmholtz} : \Delta p + k^2 p = 0 \\ \text{Dirichlet B.C.: } p_{|\partial_1\Omega} = \overline{p} \\ \text{Neumann B.C.: } v_{n_{|\partial_2\Omega}} = \dfrac{j}{\omega\rho}\dfrac{\partial p}{\partial n}|_{\partial_2\Omega} = \overline{v}_n \\ \text{mixed Robin B.C.: } v_{n_{|\partial_3\Omega}} = A_n(\omega)p \end{cases} \tag{2}$$

where c is the sound speed, $k = \frac{\omega}{c}$ is the wave number, $A_n(\omega)$ is the admittance coefficient, $\overline{v}_n$ is the prescribed velocity exciting the acoustic medium, and $\overline{p}$ is the imposed pressure on boundary $\partial_1\Omega$. In what follows, the frequency dependence of the admittance coefficients will not be written explicitly and the notation A_n will be used.

Principles of the CLE and its application to acoustics are explained in Decouvreur et al. (2004). Here is a short summary of what is necessary to understand the following developments. The idea is to split the available information into reliable and less reliable data. It is assumed that the reliable equations are the Helmholtz wave equation in the frequency domain, the Dirichlet boundary condition, and the Neumann boundary condition. It has to be noticed though, that what is called reliable or less reliable depends on each application.

The less reliable data considered in the present work is the admittance boundary condition describing the sound absorption in porous media. Indeed, different models exist to approximate the wall absorption, but none is completely reliable. The less reliable information yields a residue that is the constitutive law error estimator. Updating a setup then consists in finding the admissible pressure field minimizing the CLE.

2.2 Definition of the CLE

The CLE is an error measuring the satisfaction of the less reliable information. The CLE ξ_ω^2 measuring the modeling error at angular frequency ω is given here by:

$$\xi_\omega^2(p, v_n) = \omega^2\rho^2 \int_{\partial_3\Omega} (v_n - A_n p)^*(v_n - A_n p) d\Gamma \tag{3}$$

where p, v_n are independent fields on $\partial_3\Omega$. The relative error for each frequency ω is obtained by dividing the CLE ξ_ω^2 by the following quantity that normalizes the error:

$$\sigma_\omega^2 = \frac{\omega^2\rho^2}{2} \int_{\partial_3\Omega} ((A_n p)^* A_n p + v_n^* v_n) d\Gamma \tag{4}$$

The relative modified CLE is then written $e_\omega^{rel} = \xi_\omega/\sigma_\omega$.

2.3 The modified CLE

Since we want to update a continuous model with reference to experimental measurements, an additional measurement error is added to the error ξ_ω caused by the model formulation itself. Just as for the model, it is useful to define the reliable and less reliable equations for the measurements and to build an error measure on the less reliable experimental quantities. Measurement errors are among others due to the positioning of the sensors and microphones, their accuracy, calibration, measurement orientation,...
If we are dealing with pressure measurement by using microphones and we assume that only the measured amplitudes are less reliable, then the relative modified CLE is written:

$$e_\omega^{rel} = \left(\frac{\xi_\omega^2}{\sigma_\omega^2} + \frac{r}{1-r} \frac{\|\Pi p - \tilde{p}\|^2}{\|\tilde{p}\|^2} \right)^{1/2} \tag{5}$$

2.4 Discrete updating problem

Approximated pressure variables (P, Q) are defined as follows on $\partial_3\Omega$:

$$p = P \tag{6}$$
$$v_n = A_n Q \tag{7}$$

A variational formulation of equations (2) allows the discretization of the acoustic problem where nodal unknowns $\mathbf{P}$, $\mathbf{Q}$ are associated to pressure fields P, Q.

$$[\mathbf{K}]\mathbf{P} + j\omega\rho[\mathbf{C}]\mathbf{Q} - \omega^2[\mathbf{M}]\mathbf{P} = [\mathbf{E}]\mathbf{P} \tag{8}$$

where

- $p^h = \mathbf{N}^t\mathbf{P}$ is the approximate pressure,
- $[\mathbf{M}] = \dfrac{1}{c^2} \displaystyle\int_\Omega \mathbf{N}^t\mathbf{N} d\Omega$ is the mass matrix,
- $[\mathbf{K}] = \displaystyle\int_\Omega \nabla^t\mathbf{N}\nabla\mathbf{N} d\Omega$ is the 'stiffness' matrix,

- $[\mathbf{C}] = \int\limits_{\partial_3\Omega} A_n \mathbf{N}^t \mathbf{N} d\Gamma$ is the admittance matrix,
- $[\mathbf{E}] = \int\limits_{\partial_2\Omega} {\nabla_n}^t \mathbf{N}\mathbf{N} d\Gamma$ is the system excitation matrix due to normal velocities prescribed on boundary $\partial_2\Omega$.

The modeling CLE (3) is written for the discretized system :

$$\xi_\omega^2(\mathbf{P},\mathbf{Q}) = \rho^2\omega^2(\mathbf{Q}-\mathbf{P})^*[\mathbf{D}](\mathbf{Q}-\mathbf{P}) \tag{9}$$

where $[\mathbf{D}] = \int\limits_{\partial_3\Omega} A_n^* A_n \mathbf{N}^t \mathbf{N} d\Gamma$
The discrete form of the modified CLE (5) taking into account the experimental error is given by:

$$e_\omega^2 = \xi_\omega^2 + \frac{r}{1-r}\{\mathbf{\Pi P} - \tilde{\mathbf{P}}\}^*[\mathbf{G_w}]\{\mathbf{\Pi P} - \tilde{\mathbf{P}}\} \tag{10}$$

where $[G_w]$ represents the error measure $\|.\|^2$, Π is a projection operator that gives the value of the pressure at the corresponding sensors, $\tilde{p}$ is the measured pressure, and $\tilde{\mathbf{P}}$ the corresponding nodal value vector.
A projection operator $\mathbf{\Pi}$ is a matrix defined by:

$$\begin{cases} \Pi_{ii} = 1 \text{ if the dof } i \text{ is measured} \\ \Pi_{ii} = 0 \text{ if the dof } i \text{ is not measured} \\ \Pi_{ij} = 0 \text{ if } i \neq j \end{cases} \tag{11}$$

In the numerical example of this paper, $[\mathbf{G_w}]$ is a square unity matrix of size equal to the number of measurements. The weighting factor $\frac{r}{1-r}$ is related to the trust that we put in the measurements with respect to the model accuracy. Reference Deraemaeker et al. (2004) shows that for usual noise level on the experimental data and modeling error, $r = 0.5$ is a good choice.
The problem to be solved is :

$$\text{Find } s_\omega\text{=}(\mathbf{P},\mathbf{Q}) \mid \begin{cases} [\mathbf{K}]\mathbf{P} + j\omega\rho[\mathbf{C}]\mathbf{Q} - \omega^2[\mathbf{M}]\mathbf{P} = [\mathbf{E}]\mathbf{P} \\ \xi_\omega^2(s_\omega) \text{ is minimum} \end{cases} \tag{12}$$

The updating process consists in solving problem (12), which is done iteratively. At each iteration, the functional e_ω^2 (10) is evaluated and compared to a required quality level e_0^2 until $e_\omega^2 \leq e_0^2$.

3 Model reduction

The minimization of e_ω^2 under the admissibility constraint is achieved here by introducing Lagrange multipliers, which leads to equation (13).

$$\frac{1}{2}(\mathbf{Q}-\mathbf{P})^*[\mathbf{C}](\mathbf{Q}-\mathbf{P}) + \frac{r}{2(1-r)}(\mathbf{\Pi P}-\tilde{\mathbf{P}})^*[\mathbf{G_w}](\mathbf{\Pi P}-\tilde{\mathbf{P}}) + \mathbf{\Lambda}^*\left\{([\mathbf{K}]-\omega^2[\mathbf{M}])\mathbf{P} + j\omega\rho[\mathbf{C}]\mathbf{Q} - [\mathbf{E}]\mathbf{P}\right\} \quad (13)$$

Problem (12) is solved by deriving equation (13) with respect to $\mathbf{P}$, $\mathbf{Q}$, and the Lagrange multiplier $\mathbf{\Lambda}$.
By eliminating the Lagrange multiplier, the previous system can be rewritten under the form of two undamped forced vibration problems, the first in $\mathbf{P}$ and the second in $(\mathbf{Q}-\mathbf{P})$:

$$([\mathbf{K}]-\omega^{\mathbf{2}}[\mathbf{M}])\mathbf{P} = \mathbf{b} - j\omega\rho[\mathbf{C}]\mathbf{Q} \quad (14)$$

$$([\mathbf{K}]-\omega^{\mathbf{2}}[\mathbf{M}])(\mathbf{Q}-\mathbf{P}) = j\omega\rho[\mathbf{C}](\mathbf{Q}-\mathbf{P}) + j\frac{\omega r}{1-r}\mathbf{\Pi}^t[\mathbf{G_w}](\tilde{\mathbf{P}}-\mathbf{\Pi P}) \quad (15)$$

where $\mathbf{b} = [\mathbf{E}]\mathbf{P}$. Such problems can be reduced using a truncated modal basis to which Krylov vectors associated to the force-like terms in the right hand side are added. This technique is inspired from paper Deraemaeker et al. (2002), that suggested the idea in the case of the structural dynamics.

3.1 Truncated modal basis

Let us consider the following classical undamped forced vibration problem at angular frequency ω, in its discrete form:

$$([\mathbf{K}]-\omega^{\mathbf{2}}[\mathbf{M}])\mathbf{P} = \mathbf{F} \quad (16)$$

For a system with N degrees of freedom, there are N pairs $(\mathbf{\Phi_i}, \omega_i)$ that verify:

$$([\mathbf{K}]-\omega_{\mathbf{i}}^{\mathbf{2}}[\mathbf{M}])\mathbf{\Phi_i} = \mathbf{0} \quad (17)$$

A truncated model basis is built by taking L eigenmodes such that for $i > L$, $\omega/\omega_i \ll 1$.
The approximation can be improved by adding to the truncated modal basis series of Krylov vectors associated with the excitation $\mathbf{F}$. The series are defined as follows:

$$[\mathbf{K}]^{-1}\left([\mathbf{M}][\mathbf{K}]^{-1}\right)^{\mathbf{k}}\mathbf{F}, \quad k = 0, 1, 2, \ldots \tag{18}$$

More details about Krylov series can be found in Qu (2001). The first term of the series is the static response of the system to the excitation $\mathbf{F}$, while the next terms represent static responses to the forces $([\mathbf{M}][\mathbf{K}]^{-1})^{\mathbf{k}}\mathbf{F}$.

3.2 Application to the reduction of problem (12)

3.2.1 Excitations in equations (14) and (15)

The right hand side of equation (14) can be split into two different contributions:

- $\mathbf{b}$ (excitation applied to the system) $= \mathbf{F_1}$
- $-j\omega\rho[\mathbf{C}]\mathbf{Q} = \mathbf{F_2}$

The right hand side of equation (15) shows also two contributions:

- $j\omega\rho[\mathbf{C}](\mathbf{Q} - \mathbf{P}) = \mathbf{F_3}$
- $j\omega\frac{r}{1-r}\mathbf{\Pi^t}[\mathbf{G_w}](\tilde{\mathbf{P}} - \mathbf{\Pi P}) = \mathbf{F_4}$

3.2.2 Approximation of the excitations

Among the excitations F_1 to F_4, only $F_1 = \mathbf{b}$ is known. The other forces are approximated in what follows. The components of $\mathbf{F_4}$ are zero except for the measured degrees of freedom. This force can be considered as the sum of unit forces $\mathbf{F_{4,i}}$ at each of the sensors:

$$\mathbf{F_4} = \sum_{i=1}^{NS} a_i \mathbf{F_{4,i}} \tag{19}$$

where NS is the number of sensors.
The vector $\mathbf{F_2}$ is a function of $\mathbf{Q}$, which can be approximated by:

$$\mathbf{Q} = [\mathbf{T_0}]\mathbf{Q_r} \tag{20}$$

$$\text{with } [\mathbf{T_0}] = [\mathbf{\Phi_1} \quad \ldots \quad \mathbf{\Phi_L} \quad [\mathbf{K}]^{-1}\mathbf{F_{4,i}} \quad \ldots \quad [\mathbf{K}]^{-1}\mathbf{F_{4,NS}}] \tag{21}$$

Neglecting the $[\mathbf{K}]^{-1}\mathbf{F_{4,i}}$ basis vectors that are a correction to the truncated modal basis $[\mathbf{\Phi}]$, $\mathbf{F_2}$ can thus be approximated by:

$$\mathbf{F_2} = \sum_{i=1}^{L} a_i [\mathbf{C}] \mathbf{\Phi_i} \tag{22}$$

This approach is similar to what is done in Bouazzouni et al. (1997), Balmès (1998) and Bobillot and Balmès (2001). Similarly with what has been done to approximate $\mathbf{F_2}$, the vector $\mathbf{F_3}$ can be expressed as:

$$\mathbf{F_3} = \sum_{i=1}^{L} b_i [\mathbf{C}] \mathbf{\Phi_i} \tag{23}$$

Since the forces $\mathbf{F_2}$ and $\mathbf{F_3}$ are made of the same basis vectors (only the multiplying coefficients are different), only one of these forces has to be considered concerning its contribution in terms of the basis vectors needed to build the reduced basis.

3.2.3 Damping matrix modification during the optimization process

During the optimization process, the damping matrix $[\mathbf{C}]$ is modified at each iteration and becomes $[\mathbf{C} + \mathbf{\Delta C}]$. The forced vibration problems are consequently modified by adding a term of the form $\mathbf{F_c} = [\mathbf{\Delta C}]\mathbf{P}$ on the right hand side. Using the same approach as in section 3.2.2, $\mathbf{F_c}$ is approximated by:

$$\mathbf{F_c} = \sum_{i=1}^{L} c_i [\mathbf{\Delta C}] \mathbf{\Phi_i} \tag{24}$$

The Robin boundary condition can be subdivided in H regions that correspond to the different absorbing material regions. Each region is characterized by an admittance coefficient $A_{n,j}$ and an admittance matrix $[\mathbf{C_j}]$ whose coefficients are zero at the nodes outside this region so that:

$$[\mathbf{C}] = \sum_{j=1}^{H} A_{n,j} [\mathbf{C_j}] \tag{25}$$

It will now be shown that the modified damping matrices $[\mathbf{\Delta C_j}]$ $(j = 1, \ldots, H)$ are proportional to the local matrices $[\mathbf{C_j}]$.
If $[.]^k$ denotes the iteration number k, equation (25) becomes:

$$[\mathbf{C}]^k = \sum_{j=1}^{H} A_{n,j}^k [\mathbf{C_j}] \tag{26}$$

Defining the damping matrix modification at iteration k by

$$[\mathbf{\Delta C}]^k = [\mathbf{C}]^{\mathbf{k}} - [\mathbf{C}]^{\mathbf{0}} \tag{27}$$

combining (26) and (27) gives

$$[\mathbf{\Delta C}]^k = \sum_{j=1}^{H} (A_{n,j}^k [\mathbf{C_j}] - \sum_{j=1}^{H} (A_{n,j}^0 [\mathbf{C_j}] \tag{28}$$

$$= \sum_{j=1}^{H} (A_{n,j}^k - A_{n,j}^0)[\mathbf{C_j}] \tag{29}$$

$$= \sum_{j=1}^{H} [\mathbf{\Delta C_j}]^k \tag{30}$$

Comparing the last two lines clearly shows that $[\mathbf{\Delta C_j}]^k$ is proportional to $[\mathbf{C_j}]$, which yields:

$$\mathbf{F_c} = \sum_{i=1}^{L} c_i [\mathbf{\Delta C}] \mathbf{\Phi_i} \tag{31}$$

$$= \sum_{i=1}^{L} \sum_{j=1}^{H} c_{ij} [\mathbf{C_j}] \mathbf{\Phi_i} \tag{32}$$

3.2.4 Model projection in the reduced space

The contributions to the excitation of the undamped vibration problems leads to build a static basis $\mathbf{T_{stat}}$. If only the first term of the Krylov series is kept, the forces $\mathbf{F_i}$ $(i = 1, \ldots, 4)$ and $\mathbf{F_c}$ yield the corresponding static basis contributions, that are expressed as follows:

$$\mathbf{F_1} \dashrightarrow \mathbf{T_{stat,1}} = \left[\quad [\mathbf{K}]^{-1} \mathbf{F_1} \quad \right] \tag{33}$$

$$\mathbf{F_2}, \mathbf{F_3} \dashrightarrow \mathbf{T_{stat,2}} = \left[\quad [\mathbf{K}]^{-1} [\mathbf{C}] \mathbf{\Phi_1} \quad \ldots \quad [\mathbf{K}]^{-1} [\mathbf{C}] \mathbf{\Phi_L} \quad \right] \tag{34}$$

$$\mathbf{F_4} \dashrightarrow \mathbf{T_{stat,4}} = \left[\quad [\mathbf{K}]^{-1} \mathbf{F_{4,1}} \quad \ldots \quad [\mathbf{K}]^{-1} \mathbf{F_{4,NS}} \quad \right] \tag{35}$$

$$\mathbf{F_C} \dashrightarrow \mathbf{T_{stat,c}} = \left[\quad [\mathbf{K}]^{-1} [\mathbf{C_1}] \mathbf{\Phi_1} \quad \ldots \quad [\mathbf{K}]^{-1} [\mathbf{C_1}] \mathbf{\Phi_L} \right. \tag{36}$$

$$\left. \ldots \quad [\mathbf{K}]^{-1} [\mathbf{C_H}] \mathbf{\Phi_1} \quad \ldots \quad [\mathbf{K}]^{-1} [\mathbf{C_H}] \mathbf{\Phi_L} \quad \right] \tag{37}$$

Finally, the static basis $\mathbf{T_{stat,2}}$ is left out because its vectors are linear combinations of the basis vectors of $\mathbf{T_{stat,c}}$. The final reduced basis for the updating system is :

$$[\mathbf{T}] = [\quad [\mathbf{\Phi}] \quad [\mathbf{T_{stat,1}}] \quad [\mathbf{T_{stat,4}}] \quad [\mathbf{T_{stat,c}}] \quad] \tag{38}$$

The reduced quantities can now be expressed as follows:

$$\mathbf{P} = [\mathbf{T}]\mathbf{P_r} \tag{39}$$
$$\mathbf{Q} - \mathbf{P} = [\mathbf{T}](\mathbf{Q} - \mathbf{P})_\mathbf{r} \tag{40}$$
$$\mathbf{b_r} = [\mathbf{T}]^\mathbf{t}\mathbf{b} \tag{41}$$
$$[\mathbf{K_r}] = [\mathbf{T}]^\mathbf{t}[\mathbf{K}][\mathbf{T}] \tag{42}$$
$$[\mathbf{M_r}] = [\mathbf{T}]^\mathbf{t}[\mathbf{M}][\mathbf{T}] \tag{43}$$
$$[\mathbf{C_r}] = [\mathbf{T}]^\mathbf{t}[\mathbf{C}][\mathbf{T}] \tag{44}$$
$$[\mathbf{\Pi_r}] = [\mathbf{\Pi}][\mathbf{T}] \tag{45}$$

Note that the basis is orthonormalized to improve the system conditioning. Note also that the reduced basis is built from undamped eigenmodes. Consequently, that basis could only be used to represent the behavior of a slightly damped system, assuming that its eigenmodes are close the one of the corresponding undamped system.

4 Numerical applications

Two applications of the technique are proposed in this section. The first test-case addresses a light model. The objective is to validate the technique feasibility and check the ability of the different contributions of the reduced basis to improve the quality of the updated results.
The second numerical application deals with a 20.000 node mesh for which projecting the initial model into a sub-space is of real interest. A detailed analysis of the updated parameters is performed along the studied frequency range.

4.1 Validation of the reduced basis on a light model

The studied setup is a simplified model of a 3D car cabin that is presented in figure (1). The finite element mesh contents 1171 nodes and 814 linear elements (69 wedges and 745 bricks), and it is excited by its firewall that vibrates with normal velocity $v_0 = 1mm/s$.
The roof of the car is covered by 5 different absorbing materials with admittance coefficients $A_{n1}, A_{n2}, A_{n3}, A_{n4}, A_{n5}$. These parameters are complex and frequency dependent and the goal is to update them by minimizing the CLE. The remaining bounding surface of the car body is assumed to be rigid.
Measurements were not performed and the reference pressure field that is used to validate the model comes from a finite element simulation with the exact value of the 5 unknown parameters. A total of 16 nodal pressures simulating

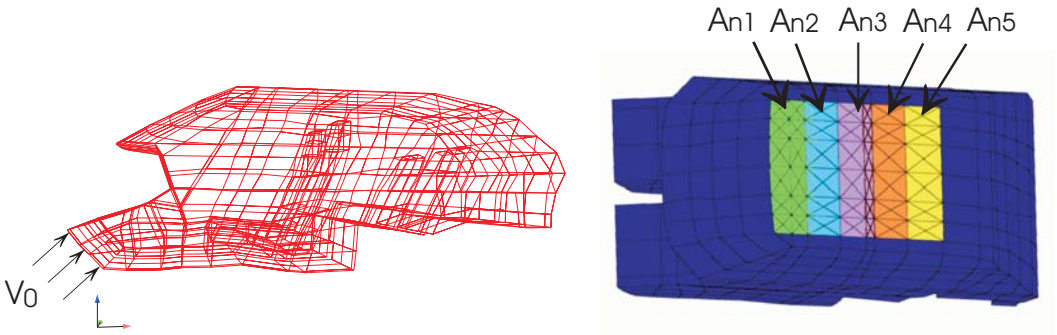

Fig. 1. Side and top view of the mesh of the light model of a car cabin

as many sensors located near the absorbing materials are taken into account. The validation of the model is achieved in the frequency range $[0-150]$ Hz with a frequency step of 2 Hz. The natural frequencies in the range $[0-300]$ Hz are presented in table 1. The initial values of the 5 admittance coefficients at the first iteration of the optimization process are set to the double of their exact values. The validation step is run using different reduced bases.
The results are reported in table (2), showing the residual CLE after validating the setup (column 2), the residual error on the 5 updated parameters, the size of the basis used (number of vectors in the basis) and the CPU-time needed to update the setup on the studied frequency range. The error levels (in %) are frequency average values. The error values on the admittance coefficients for the basis 1 explode and are therefore not mentioned.
The description of the 3 reduced bases is the following one:

- basis 1: eigenmodes in the frequency range [0-300] Hz,
- basis 2: basis 1 + $\mathbf{T_{stat,1}}$ + $\mathbf{T_{stat,c}}$,
- basis 3: basis 2 + $\mathbf{T_{stat,4}}$

Table (2) shows that a classical truncated modal basis (basis 1) is unable to simulate the behavior of the setup. Adding the static response of the system to the excitation $\mathbf{b}$ and taking into account the forces related to the system variations (basis 2) improves significantly the CLE threshold, but very low error levels on the updated parameters can only be reached by adding static responses linked to the unity vectors associated to the measured degrees of freedom (basis 3).
Finally, the residual error levels on the admittance coefficients and the CLE

64.3	137.4	183.9	221.4	261.3	280.8
107.9	151.1	189.9	244.8	269.0	286.7
118.9	158.7	217.5	260.1	277.2	294.5

Table 1
Eigenfrequencies of the light acoustic model (fig.1) in the range [0-300] Hz

Basis #	CLE [%]	A_{n1} error [%]	A_{n2} error [%]	A_{n3} error [%]	A_{n4} error [%]	A_{n5} error [%]	size(T)	CPU-time [minutes]
1	19.1	/	/	/	/	/	18	50
2	0.49	1.31	5.40	2.03	1.25	4.34	64	94
3	0.07	0.56	2.76	0.88	0.39	0.77	78	127

Table 2
Residual CLE after validating the setup (column 2), residual error on the 5 updated parameters, size of the basis used (number of vectors in the basis) and CPU-time needed to update the setup

are very low (mostly less than 1%), which is comparable to the stop criterion e_0 that is used when updating the acoustic problem with the full discrete system. So, the updating quality with the reduced basis is like the one of the full system, which validates the reduced basis.

4.2 Acoustic absorption in a car cabin

This numerical application is intended to apply the constitutive law error updating technique while using the reduced basis developed trough chapter 3 to a model with a mesh density justifying the need for the model size reduction.

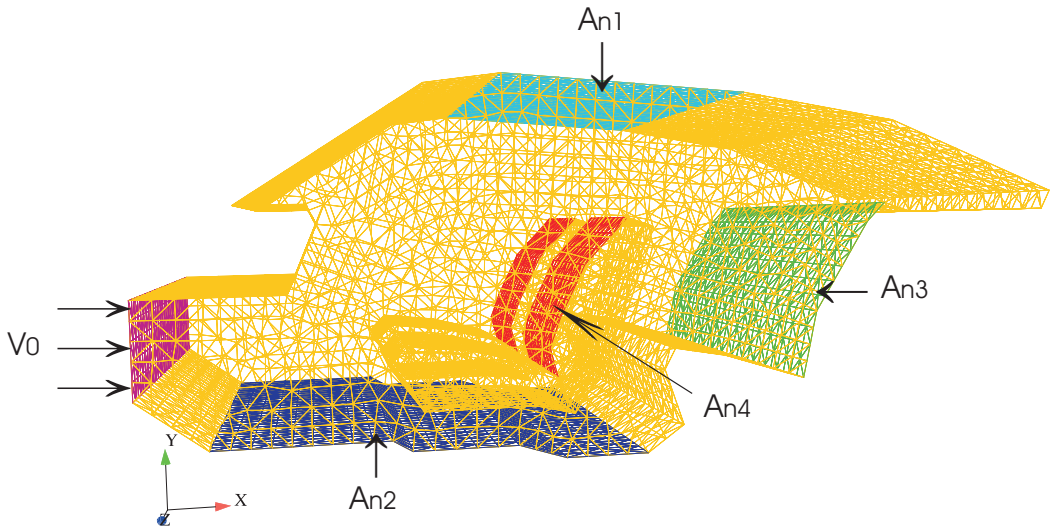

Fig. 2. Side view of the car cabin mesh and its boundary conditions

88.3	212.5	290.2	347.3	393.4	434.9	480.9	517.6	549.0	596.7
126.5	234.2	298.8	350.3	399.6	439.5	490.5	522.9	555.5	598.6
144.7	245.0	304.8	362.8	407.8	446.0	500.7	526.8	568.4	
154.6	255.9	308.9	369.6	410.9	453.6	506.4	530.6	577.8	
172.2	269.2	318.4	375.5	422.5	463.0	508.4	534.2	583.3	
192.6	277.7	323.2	381.1	426.6	464.3	514.1	538.3	589.5	
197.3	285.8	329.5	390.3	430.2	470.7	515.1	544.8	594.1	

Table 3
Eigenfrequencies of the acoustic domain of fig.2 in the range [0-600] Hz

The geometry is pretty similar to the one of the first numerical example in the sense that it represents also the acoustic domain of a car cabin. The outer shape of the setup is nevertheless somewhat different (in this case the trunk is not represented for instance) and the seat sketching was improved. The longitudinal length of the present device is also somewhat shorter, which explains why the eigenfrequencies are typically higher.
The mesh is made of 19.725 nodes and 100.087 linear tetrahedral elements. One focuses on the acoustic absorption related to the materials covering the roof, the floor and the back-rest of both the front and the rear seats of the car. Admittance coefficients correspondence is the following one:

- A_{n1} refers to the roof of the car as represented in fig.2,
- A_{n2} refers to the floor of the car,
- A_{n3} refers to the back-rest of the rear seat of the car,
- A_{n4} refers to the back-rest of the front seat.

The surface bounding the acoustic domain which is not covered by absorbing materials is assumed to be rigid, with the exception of the firewall that vibrates with a normal velocity $v_0 = 1mm/s$ and constitutes the only acoustic source. Fig. 2 highlights the geometry together with the vibrating firewall and the damping boundary conditions.
The device is updated in the frequency range [100-400] Hz and the modal basis makes use of eigenvectors up to 600 Hz. The corresponding natural frequencies of the setup are reported in table 3. The admittance coefficients are updated every 25 Hz, and the initial values of the admittance coefficients at the first iteration of the optimization process are set to the double of their exact values. The nodal pressure is recorded at 50 different locations randomly distributed into the acoustic domain to simulate the measurements.
The updating process is applied twice to the setup. During the second run, the reference finite element pressure field replacing the measurements is polluted numerically in order to simulate a slight discrepancies in the experimental data.

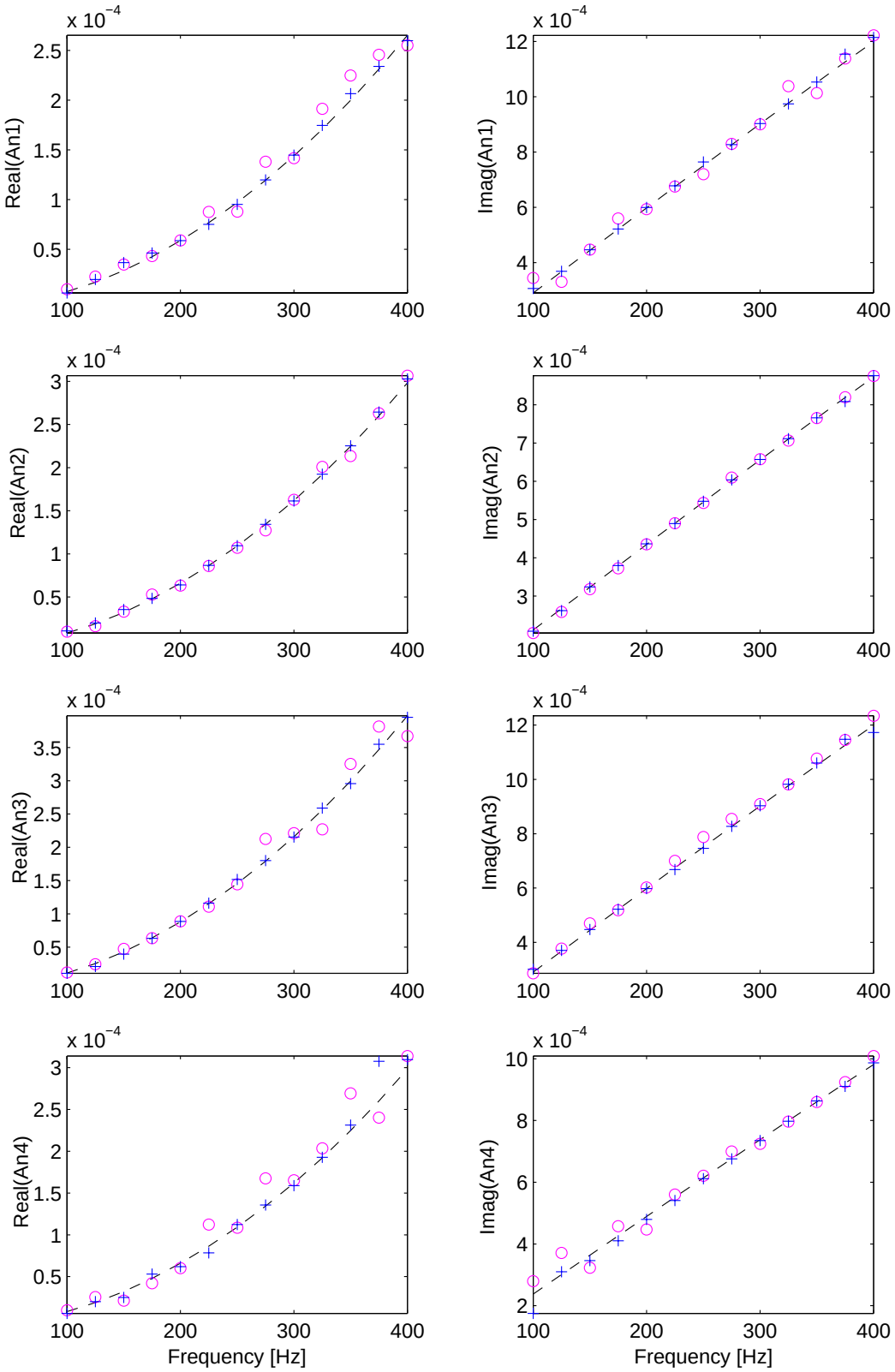

Fig. 3. Updated admittance coefficients with 5% measurement noise ('o' plot symbols) and without noise ('+' plot symbols); the dotted line draws the reference values

The noisy reference field is obtained by multiplying the real and imaginary parts of each measurement by $1+\omega*N$, where N is a random number chosen from a normal distribution with mean zero and variance one, and ω is the weight applied to the normal distribution, and so the average noise level that is set to 5%. The updated admittance parameters are plotted in fig.3. Both the real and imaginary parts of the coefficients are reported and compared to the exact values while updating the model with and without measurement noise. The corresponding errors on the admittance magnitude are shown in fig.4: the maximum error level is about 5% with perfect experimental data, and it never reaches 10% when polluting the reference pressure field. The average values over the frequency range are significantly lower.
Fig.5 draws the residual constitutive law error after updating along the frequency range of interest. The CLE varies between 1 and 8.5% with noisy measurements, and it drops significantly when using perfect experimental data.
The CPU time speedup is also plotted in fig.5. It is computed by the ratio of the running time of the full non reduced model updating process at a given frequency and the corresponding time while projecting the model into the sub-space, and this ratio moves around 110. Actually, the number of iterations needed for updating the setup at a given frequency is about the same while using the full or the reduced model (around 300 iterations). So, the speedup to update the system at each frequency is close to the ratio of the

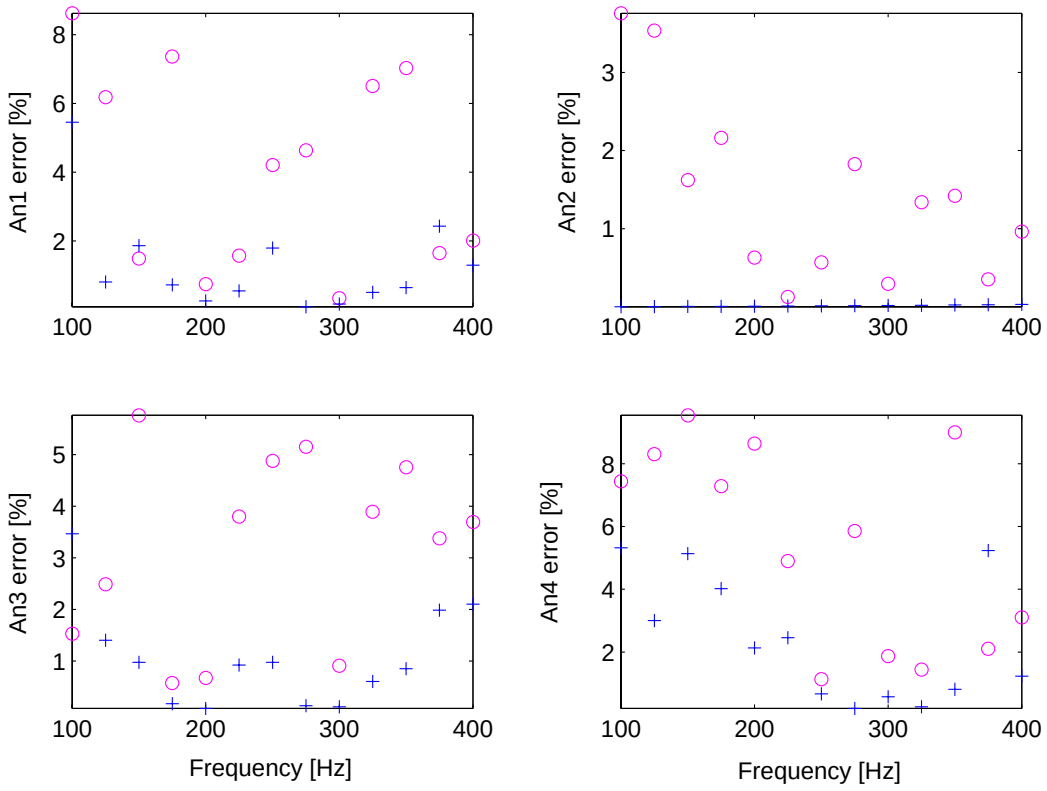

Fig. 4. Updated admittance coefficient error with 5% measurement noise ('o' plot symbols) and without noise ('+' plot symbols)

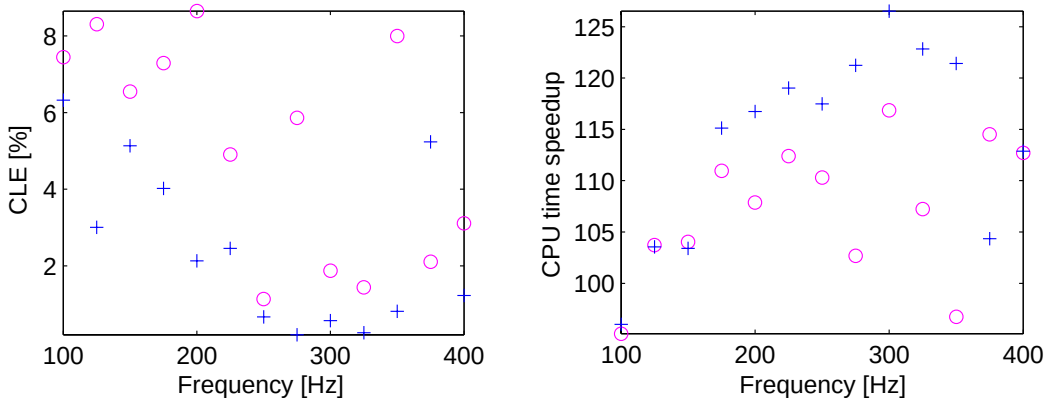

Fig. 5. CLE residue after updating and CPU time speedup (full/reduced model updating time ratio): updating with 5% measurement noise ('o' plot symbols) and without noise ('+' plot symbols)

CPU times needed to compute one single iteration with the full and the light models. Note that the full model computations are achieved in a optimized way, taking advantage of the sparse property of the finite element matrices and using a skyline solver to invert the system of equations. The initial sparse system size is 39450 (twice the number of nodes) while the reduced non-sparse equation set size is 818 (twice the number of vectors in the reduced basis).
The order of magnitude for the time needed to update the 20.000 node models on a single 2.4 GHz Linux processor is around 4 minutes for each frequency when using the reduced basis. It yields to somewhat less than one hour to update the system in the [100-400] Hz frequency range with an increment of 25 Hz. With a deceleration of ca. 110, the entire non reduced model updating process runs for four days.

5 Conclusions

The paper discusses the problem of validating large acoustic setups of industrial size by the mean of the constitutive law error technique. In order to update such models, the optimization problem is rewritten under the form of a system of undamped forced vibration problems.
That leads us to build a reduced basis with the following contributions:

- a truncated modal basis,
- the static response of the system to the excitation of the acoustic domain (Krylov series),
- static responses to the forces related to the variations of the system during the updating process,
- static responses associated to the measured degrees of freedom

The reduced basis is implemented and tested on two numerical examples. The paper presents a very simplified model of a 3D car cabin: the updating of the model is achieved using 3 different bases, the first being a classical truncated modal basis, and the others adding progressively the static contributions listed above. Comparing the results of the 3 validations shows that a very good quality for the updating process is only reached when the reduced basis is used with all the contributions proposed in the paper.
A second application deals with a pretty similar geometry but with a refinement of about 20.000 nodes. The absorbing materials covering the roof, the floor and the the back-rest of both the front and the rear seats of the car are updated with and without measurement noise. A detailed analysis of the numerical results is presented. Compared to the validation step that uses the full non reduced model, the CPU-time of the reduced updating process is about 110 times lower for this setup of average size.

Acknowledgements

The research on the building of a reduced basis adequate for the updating of acoustic models with the CLE technique was conducted in the context of a study stay at the Laboratoire de Mécanique et Technologie, Cachan/Paris.
The financial support of the Fonds National de la Recherche Scientifique (Belgium) is gratefully acknowledged.

References

Balmès, E., 1996. Parametric families of reduced finite element models, theory and applications. In: Mechanical Systems and Signal Processing. Vol. 10 (4). pp. 381–394.

Balmès, E., 1998. Efficient sensitivity analysis based on finite element model reduction. In: Proc. IMAC XVII, SEM, Santa Barbara, CA.

Bobillot, A., Balmès, E., 2001. Solving minimum dynamic residual expansion and using results for error localisation. In: Proc. IMAC XIX, SEM, Kissimee, Florida.

Bouazzouni, A., Lallement, G., Cogan, S., 1997. Selecting a ritz basis for the reanalysis of the frequency response functions of modified structures. In: Journal of Sound and Vibration. Vol. 2. pp. 309–322.

Bui, Z., 2002. Krylov subspace techniques for reduced order modelling of large-scale dynamical systems. In: Applied Numerical Math. Vol. 43. pp. 9–44.

Burnett, D. S., 1994. A three-dimensional acoustic finite element based on a prolate spheroidal multipole expansion. In: J. Acoust. Soc. Am. Vol. 96. pp. 2798–2816.

Decouvreur, V., Bouillard, P., Deraemaeker, A., Ladevèze, P., 2004. Updating 2d acoustic models with the constitutive relation error. In: Journal of Sound and Vibration. Vol. 278(4/5). pp. 773–787.

Deraemaeker, A., Ladevèze, P., Leconte, P., 2002. Reduced bases for model updating in structural dynamics based on constitutive relation error. In: CMAME 191(21-22).

Deraemaeker, A., Ladevèze, P., Romeuf, T., 2004. Model validation in the presence of uncertain epxerimental data. In: Engineering Computations. Vol. 21-8. pp. 808–833.

Freund, R. W., 2000. Krylov-subspace methods for reduced order modelling in circuit simulation. In: J. Comput. Appl. Math. Vol. 123. pp. 395–421.

Ladevèze, P., 1998. A modelling error estimator for dynamic model updating. In: New Advances in Adaptative Computational Methods in Mechanics. Elsevier, pp. 135–151.

Qu, Z., 2001. Accurate methods for frequency responses and their sensitivities of proportionally damped systems. In: Computers&Structures. Vol. 79. pp. 87–96.

Rohl, P., Reese, G., 2000. Salinas - an implicit finite element structural dynamics code developed for massively parallel platforms. In: American Institute of Aeronautics and Astronautics. pp. 1651–1660.

Tournour, M., Atalla, N., 1999. Efficient evaluation of the acoustic radiation using multipole expansion. In: Int. J.Num. Meth. Engrg. Vol. 46 (6). pp. 825–837.